

Correlation energy functionals for *ab initio* calculations: Application to transition metals

N. E. Zein

Russian Research Centre "Kurchatov Institute," Moscow, 123182, Russia

(Received 14 March 1995; revised manuscript received 16 June 1995)

The method for including strong correlation effects in self-consistent electronic structure calculations in solids is presented. On the basis of the mean-field-type (Gutzwiller-type) approximation the correlation energy functional is obtained, which depends on the partial electron density. In turn, the variation of this functional yields the nonlocal effective potential. Two possible variational procedures are tested: variation of the functional over occupation numbers only and over both occupation numbers and linear-muffin-tin-orbital-atomic-sphere-approximation (LMTO-ASA) wave function. The LMTO-ASA calculations for a number of *3d* and *4d* transition metals are carried out. The results are compared with those for density-functional calculations. Quantitative estimates of the correlation renormalization factor for the bandwidth "dynamical" narrowing in these metals are presented.

I. INTRODUCTION

The density-functional (DF) method, especially its local-density approximation (LDA) and spin-dependent counterparts (LSDA), is the basis for realistic electronic structure calculations in solids. In most cases the calculated cohesive energy and its derivatives, such as the pressure at the experimental unit cell volume, elastic moduli, and even phonon spectra are in excellent agreement with the experiment. Nevertheless, a number of example of LDA failure are known. They can be approximately divided into three groups. The first case includes atom and surface calculations where the main error arises due to the wrong asymptote of the LDA potential—it falls off exponentially instead of as $1/r$. The second case is the band gap in semiconductors and dielectrics. Though band dispersion is an auxiliary notion for the DF method and formally it should not coincide with the experiment, usually such a coincidence takes place in metals. The strong discrepancy in band gap values also makes one seek for LDA improvement. The third case is the case of substances with strong electron on-site repulsion, e.g., *3d* transition metals, transition metal oxides, high- T_c superconductors (HTS's), and *f* metals. It is generally accepted that the first and second cases are mainly connected with the wrong long-distance asymptote of the LDA potential and various methods to improve it are used: self-interaction corrected (SIC)-LDA, the corrected gradient (GCA) method, the *GW* approximation, a combination of LDA and Hartree-Fock methods.¹ The third case is directly connected with strong correlation effects. The importance of such effects, when the electron on-site repulsion U exceeds or equals the mean conductive bandwidth W , is well-known from Hubbard or Anderson model investigations. Below, one of the possible approaches to the problem of incorporating strong correlation effects in *ab initio* calculations will be discussed.

Few techniques used for this purpose are known.

The most developed approach, widely tested for metal oxides² and HTS's,³ is the LDA+ U approach.⁴ This approach is based on LDA calculations in the paramagnetic phase and greatly improves results in phases with magnetic ordering in comparison with the LSDA approach. This approach was first suggested for the impurity case and it provided the true values of impurity level splitting, when compared with the results of photoemission experiments.⁴ Later,^{2,3} it was used for finding excitation spectra and gaps in regular crystals. One of the merits of the LDA+ U method is the accurate calculation of U , which takes into account screening and exchange effects. But in the case of a paramagnetic regular crystal the LDA+ U method ground state energy should coincide with that in the LDA approach.

The second approach,⁵⁻⁷ which below will be called the short-range correlation (SRC) functional approach, directly deals with the effective Hamiltonian of the Hubbard or Anderson model. The parameters of these Hamiltonians are calculated self-consistently with the wave functions, which are the solutions of the Schrödinger equation with an effective potential. The ground state energy calculated with the model Hamiltonian gains additional corrections due to correlation effects. The correlation energy obtained so far in turn is varied over occupation numbers or wave functions to obtain an effective potential in the spirit of general DF theory ideas. Such an approach was applied to finding excitation spectra in the one-dimensional model⁵ and in the transition metals Fe, Co, and Ni.⁶ The influence of correlations on the equilibrium unit cell volume and bulk modulus for transition metals in the paramagnetic phase was also discussed in the framework of this method.⁷ One of the reasonable approximations for finding the correlation energy in the Hubbard model can be used. The "second order in U " approximation⁸ was used in Refs. 5 and 6 meanwhile in Ref. 7 it was a variant of the Gutzwiller approximation⁹⁻¹¹ for d electrons, with the effective repulsion constant $U = f_{ss}^0 + f_{dd}^0 - 2f_{sd}^0$, where f_{ij}^0 are the

matrix elements of the Coulomb interaction between electrons with angular momenta l and l' . Both LDA+ U and SRC approaches have their drawbacks and merits. The drawback of the SRC approach is the indirect assumption that the correlation effects are manifest mainly in occupation number variation; meanwhile the wave functions are approximately the same in various atomic configurations. The confirmation of this assumption for pure metals will be discussed in Sec. III. The second item which demands further development is the inclusion of screening effects in the effective interaction V_λ between electrons. The problem can hardly be solved in terms of one-site interaction constants, but one of the possible approaches to finding V_λ is presented in Appendix C. But in contrast to the LDA+ U method the energy in the SRC approach is a mean value of the full Hamiltonian in its ground state even in the paramagnetic phase. A similar technique was also used for finding the electronic structure¹² of small clusters of Pb atoms with a local ansatz,¹³ but the matrix elements of the effective Hamiltonian¹² were not calculated self-consistently, in contrast with the present approach.

Below we shall discuss just the paramagnetic phase ground state in the framework of the SRC approach. In this case a number of interesting and yet unexplained effects exist even at the level of equilibrium lattice properties, such as the bulk modulus and unit cell volume. There is a well-known cusp for unit cell volume and bulk modulus values in the middle of the 3d metal row; abnormally low bulk modulus values in intermetallic $Zr_{2-x}V_{1+x}$ compounds with a strong dependence on concentration x , abnormally low bulk modulus in $Sm_{0.75}Y_{0.25}S$ in comparison with the Vegard law value, bulk modulus decreasing in Mn-Cu alloys, etc. Indirect indications, such as the appearance of magnetic order under slight variation of parameters, make one feel that in this case we deal with a manifestation of the effects of strong correlations in the paramagnetic phase. The present approach differs from the preliminary version⁷ in two respects. First, on-site correlations of both s, p and d electrons are considered on an equal footing in the framework of the generalized Gutzwiller approach. Though in the case of s and p electrons the screening effects give the main contribution in correlation energy and on-site correlation effects are negligible, as is shown in Sec. III, their inclusion in the Gutzwiller-type wave function is important from another point of view. The on-site repulsion interaction constants f_{ii}^0 exceed the constant U , which is the difference between sp and d constants, especially for the “bare” Coulomb interaction (10–20 eV against 5–10 eV). Thus it is more profitable to leave the number of electrons at the atom unchanged, but to replace the d electron with an s electron. As a consequence a new internal degree of freedom appears, which is absent in the homogeneous electron gas and which is connected with the difference between the repulsion of sp and d electrons. For this reason only d electrons are usually considered in the Hubbard model and the interaction of these electrons is reduced to a constant U . The inclusion of both d and sp electrons in the Hamiltonian and generalized Gutzwiller ansatz permits one to realize the above-

mentioned model: the most advantageous neutral configurations are now selected automatically and the amount of charged configuration at every atom is also selected by energy minimization. In this sense the U value forms now in the process of the calculations. Secondly, the variational procedure is applied to variation over both occupation numbers and wave functions. It permits one to remove *ad hoc* assumptions and to make the approach in principle self-contained and checked. The paper is organized as follows. In Sec. II the main topics inevitably arising when one is trying to distinguish the short-range correlation energy contribution are discussed. These items are the exchange and correlation contributions in metals, the values and form of the short-range interactions, valence-core partitioning, the mean-field approximation for the correlation energy of s , p , and d electrons, variational equations, and effective potentials. Expressions for the correlation contribution in some limiting cases are derived. In Sec. III linear-muffin-tin-orbital-atomic-sphere-approximation (LMTO-ASA) results for 3d metals both in the middle of the row (V, Mn) and at the end of the row (Cu, Ni) are listed. They are compared with the DF results and with the results for their analogs from the 4d row. The values of on-site repulsion and band narrowing factor for these metals are presented. In the Conclusion further generalizations of the method are discussed, which seem to demand the introduction of a model Hamiltonian with interaction between neighboring lattice sites.

II. SHORT-RANGE CORRELATION ENERGY FUNCTIONAL IN LMTO-ASA CALCULATIONS

As noted in Ref. 7, the value of the interaction constant U

$$U = f_{dd}^0 + f_{ss}^0 - 2f_{sd}^0, \\ f_{ii}^L = \int_0^{R_{ws}} |\psi_i(r)|^2 \int_0^{R_{ws}} |\psi_{i'}(r')|^2 \frac{r_{<}^L}{r_{>}^{L+1}} dr dr', \quad (1)$$

where $r_{>}$ and $r_{<}$ are the minimum and maximum values of r and r' and $\phi_i(r)$ are the wave functions, can be used as an estimation of the importance of the on-site repulsive correlations effects. In 3d metals this value increases from 1.5 eV in V to 7.5 eV at the end of the row. In 4d metals it constitutes about 1 eV and approximately coincides with that in the free electron gas. For this reason the maximum effect will be in the middle of the 3d row, as the number of electrons (holes) diminishes at the end of the row. The aim of the developed technique is to incorporate this crude effect in the *ab initio* ground state energy calculations. To be more concrete, we shall start with the LMTO-ASA method, which is the most “natural” for this purpose, as its wave function is approximately factorized on the \mathbf{k} -dependent coefficient $A_{\mathbf{k}L}^\nu$ and \mathbf{r} -dependent wave function $Y_{lm}(\hat{r})\phi_l(r)$ inside each cell. $\phi_l(r)$ is the solution of the radial Schrödinger equation with a potential $U(r)$:

$$[\hat{T} + U(r)]\phi_l(r) = \varepsilon_l \phi_l(r), \quad \dot{\phi}_l(r) = \frac{d\phi_l(r)}{d\varepsilon_l}, \quad (2)$$

where \hat{T} is the kinetic energy operator and usually $U(r)$ is chosen to be the LDA potential. Complete factorization would reduce the problem to a Hubbard model on the lattice with known hopping integrals between various sites and a model interaction Hamiltonian which can be solved by various approximate methods. The correlation energy thus obtained in turn depends on the occupation numbers Q_L and functions $\phi_l(r)$. Its variation over Q_l will bring about an effective potential in addition to the usual DF potential, which takes into account the on-site repulsion. The weak (for d electrons) \mathbf{k} dependence of the MTO's introduces further approximations, but in principle the procedure remains the same.

A. LMTO-ASA basis set and effective Hamiltonian

In the present work an energy-independent MTO basis set¹⁴ is used which is convenient for the variational approach to the one-electron eigenvalue problem. The MTO's smoothly match each other on the Wigner-Seitz sphere with the radius R_{WS} while the coefficients $A_{\mathbf{k}L}^\nu$ can be found from the secular equation corresponding to the minimum of the one-electron energy E_0 . In the LMTO-ASA method the decomposition of the Bloch wave function $\Psi_{\mathbf{k}}^\nu(\mathbf{r}) = \sum_L \Psi_{\mathbf{k}L} A_{\mathbf{k}L}^\nu$ inside the unit cell is known to be¹⁴

$$\Psi_{\mathbf{k}L}(\mathbf{r}) = \sum_{L'} \frac{i^{l'} Y_{L'}(\hat{r})}{r} [\phi_{l'}(r) \delta_{LL'} + h_{\mathbf{k},L}^{\mathbf{k}'} \phi_{l'}(r)], \quad (3)$$

where $L = \{lm\}$ and standard¹⁴ LMTO coefficients $h_{\mathbf{k},L}^{\mathbf{k}'}$ are introduced. For convenience the expressions for the $\hat{h}^{\mathbf{k}}$ matrix elements in terms of the $\phi_l(R_{WS})$ values are listed in Appendix A. The energy functional $E_0[A_{\mathbf{k}L}^\nu]$, which has the minimum at the orthonormalized set of $\Psi_{\mathbf{k}}^\nu$, is a quadratic form in coefficients $a_{\mathbf{k}}^\nu = \hat{W}^{+\mathbf{k}} A_{\mathbf{k}}^\nu$:

$$\begin{aligned} E_0[a_{\mathbf{k}L}^\nu] &= \langle \Psi_0 | (\hat{T} + U) | \Psi_0 \rangle \\ &= \sum_{LL'} a_{\mathbf{k}L}^\nu H_{LL}^{\mathbf{k}} a_{\mathbf{k}L'}^\nu \theta_{\mathbf{k}}^\nu, \end{aligned} \quad (4)$$

with the normalization condition

$$\sum_{LL'} A_{\mathbf{k}L}^{*\nu} O_{LL'}^{\mathbf{k}} A_{\mathbf{k}L'}^\nu = \sum_L a_{\mathbf{k}L}^{*\nu} a_{\mathbf{k}L}^\nu = \delta_{\nu\nu'}$$

Expressions for $\hat{H}^{\mathbf{k}}$ and $\hat{O}^{\mathbf{k}} = \hat{W}^{\mathbf{k}} \hat{W}^{+\mathbf{k}}$ in terms of the matrix $\hat{h}^{\mathbf{k}}$ are also listed in Appendix A. $|\Psi_0\rangle$ is the ground state of noninteracting electrons and $\theta_{\mathbf{k}}^\nu$ is the Fermi step function. It is also convenient to distinguish in Eq. (4) terms corresponding to hopping onto other sites:

$$T_{LL'}^{\mathbf{k}} = H_{LL}^{\mathbf{k}} - \sum_{\mathbf{k}} H_{LL'}^{\mathbf{k}}. \quad (5)$$

Starting with Eq. (4) the Hamiltonian can be expressed

in terms of creation $\hat{c}_{\mathbf{k}}^{\dagger\nu}$ and annihilation $\hat{c}_{\mathbf{k}}^\nu$ operators. With $\hat{c}_{L\mathbf{k}} = \sum_\nu a_{\mathbf{k}L}^\nu \hat{c}_{\mathbf{k}}^\nu$ the Hamiltonian of noninteracting electrons is

$$\hat{H}_0 = \sum H_{LL}^{\mathbf{k}} \hat{c}_{\mathbf{k}L}^\dagger \hat{c}_{\mathbf{k}L}.$$

The electron density $\rho(r)$ is expressed in the LMTO-ASA as $\sum_{\alpha\beta} q_l^{\alpha\beta} \phi_l^\alpha(r) \phi_l^\beta(r) / 4\pi r^2$ with

$$q_l^{\alpha\beta} = \sum_{\{L_i\}\mathbf{k}} \theta_{\mathbf{k}}^\nu A_{L_1\mathbf{k}}^{*\nu} A_{L_2\mathbf{k}}^\nu h_{LL_1}^{\alpha\mathbf{k}} h_{LL_2}^{\beta\mathbf{k}},$$

where $\phi_l^\alpha(r)$ and $h_{LL}^{\alpha\mathbf{k}}(r)$ are defined in Appendix A. The number of electrons in state l is

$$q_l = \int \sum_{\alpha\beta} q_l^{\alpha\beta} \phi_l^\alpha(r) \phi_l^\beta(r) dr = q_l^{00} + q_l^{11} \langle \phi_l^2 \rangle. \quad (6a)$$

It is also convenient to define the value Q_L

$$Q_L = \langle \Psi_0 | \hat{n}_L | \Psi_0 \rangle, \quad \hat{n}_L = \frac{1}{N} \sum_{\mathbf{k}} \hat{c}_{\mathbf{k}L}^\dagger \hat{c}_{\mathbf{k}L}, \quad (6b)$$

which is close to q_l in metals.

Let us suppose for a while that only terms with \mathbf{R} in one and the same unit cell exist in the interaction Hamiltonian and the matrix elements of the interaction between the wave functions Eq. (3) are \mathbf{k} independent. Then the Hamiltonian has the form of a multiband Hubbard model with various interaction constants $f_{ll'}$ between l and l' electrons: $\hat{H} = \hat{H}_0 + \hat{H}_{\text{int}}$.

$$\hat{H}_{\text{int}} = \frac{1}{2} \sum f_{ll'}^L C_{lm_1 m_4}^{*LM} C_{l'm_2 l' m_3}^{LM} \hat{c}_{lm_1}^\dagger \hat{c}_{l'm_2}^\dagger \hat{c}_{l' m_3} \hat{c}_{lm_4} \quad (7)$$

with $C_{lm_1 m_4}^{LM} = \int Y_{lm}^*(\theta, \varphi) Y_{LM}(\theta, \varphi) Y_{lm}(\theta, \varphi) d\omega$.

B. Gutzwiller approximation for the ground state energy

A number of reasonable and carefully tested approximations exist for finding the ground state energy with a Hamiltonian of such a type. Below we shall use the Gutzwiller approximation,⁹⁻¹¹ which is a mean-field version of the Gutzwiller-wave function approximation and the saddle-point limit of the slave-boson method.¹¹ In most cases it has an accuracy of a few percent when compared with quantum Monte Carlo calculations.^{10,11} The many-body wave function in this approximation has the factorized form

$$\begin{aligned} |\Psi\rangle &= \prod_{\mathbf{R}} \frac{1}{K_{0\mathbf{R}}^{1/2}} \hat{U}_{\mathbf{R}} |\Psi_0\rangle, \\ \hat{U}_{\mathbf{R}} &= \exp \left(- \sum_j \gamma_j \hat{O}_{j\mathbf{R}} - \sum_L \mu_L \hat{n}_{L\mathbf{R}} \right), \end{aligned} \quad (8)$$

where $\hat{O}_{j\mathbf{R}}$ are two-particle operators and γ_j are the variational parameters. $K_{0\mathbf{R}} = \langle \Psi_0 | \hat{U}_{\mathbf{R}} \hat{U}_{\mathbf{R}} | \Psi_0 \rangle$ is the

normalization constant. For the s -electron Hubbard model $\hat{O} = \hat{n}_\downarrow \hat{n}_\uparrow$, to exclude states with double occupation of the same atom. In the local ansatz proposed by Stolhoff and Fulde,¹³ which is close in spirit to the Gutzwiller approximation, several operators \hat{O}_j corresponding to the most important correlations are taken into account. It seems that the most natural choice of \hat{O} consists in taking \hat{O} equal to \hat{H}_{int} ,⁷ as in this case the functions $\hat{O}^n |\Psi_0\rangle$ are linear combinations of Lanczos wave functions, which provide the best variational subspace for low-lying excitations.¹⁵ Of course, due to the finite dimension of the subspace at each site, 2^{N_i} with $N_i = 2(2l + 1)$, any form of \hat{U} with the necessary number of variational parameters is suitable, but in practice only one or two parameters are used and in this case the choice $\hat{O} = \hat{H}_{\text{int}}$ is preferable. The renormalization con-

stants μ_L are found from the condition of conservation of electron numbers Q_L [Eq. (6b)]:

$$Q_L = \langle \Psi | \hat{n}_L | \Psi \rangle. \quad (9)$$

For practical calculations it is convenient to expand \hat{U} over projection operators corresponding to n filled states λ_i and m empty states η_j :

$$\hat{P}_{nm} = \prod \hat{n}_{\lambda_1} \cdots \hat{n}_{\lambda_n} (1 - \hat{n}_{\eta_1}) \cdots (1 - \hat{n}_{\eta_m}). \quad (10)$$

The ground state energy is the Hamiltonian averaged over the ground state wave functions and after subtracting $E_0 = \langle \Psi_0 | \hat{H}_0 | \Psi_0 \rangle$ the exchange-correlation energy has the form¹¹

$$E_{\text{XC}}^s = - \sum_{\mathbf{k}LL'} T_{LL'}^{\mathbf{k}} (1 - \xi_L \xi_{L'}) \langle \hat{c}_{\mathbf{k}L}^\dagger \hat{c}_{\mathbf{k}L} \rangle_0 + \frac{1}{2} \sum_{L_1 L_2} f_{l_1 l_2}^0 \langle \Psi | (\hat{n}_{L_1} - Q_{L_1}) (\hat{n}_{L_2} - Q_{L_2}) | \Psi \rangle - \frac{1}{2} \sum_L f_{ll}^0 Q_L + \frac{1}{2} \sum_{\substack{L=2,4 \\ \{m_i\}}} f_{ll'}^{LM} C_{lm_1 m_4}^{*LM} C_{l'm_2' m_3}^{LM} \langle \Psi | \hat{c}_{lm_1}^\dagger \hat{c}_{l'm_2'}^\dagger \hat{c}_{l'm_3} \hat{c}_{lm_4} | \Psi \rangle, \quad (11)$$

where $T_{LL'}^{\mathbf{k}}$ is defined by Eq. (5) and the renormalization factor ξ_L arises in the Gutzwiller approximation as the weight of averaging over all electron configurations, except those with the L electron:

$$\xi_L = \langle \Psi_0 | \hat{U}_{1L} \hat{U}_{2L} | \Psi_0 \rangle, \quad (12)$$

where \hat{U}_{1L} and \hat{U}_{2L} do not contain L operators: $\hat{U} = \hat{n}_L \hat{U}_{1L} + (1 - \hat{n}_L) \hat{U}_{2L}$. The L electron in this approximation is pairing with electron L' on the other lattice site.^{9,11} For this reason only part of the one-electron energy H_0 , corresponding to distant hopping, is presented in $T_{LL'}$. On-site one-electron terms are not changed in accordance with Eq. (9). The ξ_L is the measure of dynamical band narrowing due to correlations and the mean occupancy of states with $\varepsilon_{\mathbf{k}}^\nu < \varepsilon_F$ is now $(1 + \xi_L^2)/2$ and with $\varepsilon_{\mathbf{k}}^\nu > \varepsilon_F$ is $(1 - \xi_L^2)/2$.⁹ ξ_L values of about 0.5–0.7 correspond usually to a phase transition to the dielectric or some other possible phase. As noted in a number of works, the Gutzwiller approximation, which corresponds to ξ_l values independent of $(\varepsilon - \mu)$, is not reliable near phase transitions. But, as we shall see in Sec. III, in 3d metals the minimum ξ_d value is approximately 0.9 in Mn, i.e., it is far from a possible Mott-Hubbard transition. For the full interaction Hamiltonian, the U decomposition over operators P_{nm} from Eq. (10) should be done numerically, by finding the H_{int} eigenvectors. But with $f^{2,4} = 0$ and $\langle \hat{n}_L \rangle$ values independent of M , which is a good approximation for metals with cubic symmetry, the form of U is significantly simplified. In the last case, it is convenient to deal with operators $\hat{Q}_l = \sum_m \hat{n}_{lm}$ and their mean value is $Q_l = \langle \hat{Q}_l \rangle$. The one-site contribution to the correlation energy E_c^s has the form

$$E_c^s = - \sum_{\mathbf{k}LL'} T_{LL'}^{\mathbf{k}} (1 - \xi_L \xi_{L'}) \langle \hat{c}_{\mathbf{k}L}^\dagger \hat{c}_{\mathbf{k}L} \rangle_0 + \frac{1}{2} \sum_{ll'} f_{ll'}^0 \langle \Psi | (\hat{Q}_l - Q_l) (\hat{Q}_{l'} - Q_{l'}) | \Psi \rangle - \frac{1}{2} \sum_l f_{ll}^0 Q_l + \frac{1}{2} \sum_l f_{ll}^0 \frac{Q_l^2}{N_l}, \quad \xi_l = \frac{1}{N_l} \sum_{m,\sigma} \xi_{lm\sigma}, \quad \hat{U} = \exp \left(-\gamma \sum_{ll'} f_{ll'}^0 (\hat{Q}_l - Q_l) (\hat{Q}_{l'} - Q_{l'}) - \sum_l \mu_l \hat{Q}_l \right), \quad (13)$$

and decomposition of \hat{U} operators over \hat{P}_{nm} operators can be done by hand (see Appendix B). All crude effects such as stronger repulsion of d electrons than s or p electrons or the unprofitableness of charged configurations are still present in \hat{U} defined by Eq. (13). For this reason \hat{U} automatically selects configurations with the total number of electrons equal to that in atom. The term $-\frac{1}{2} \sum_l f_{ll}^0 \frac{Q_l^2}{N_l}$ corresponding to exchange diagrams is singled out and the rest are gathered in the correlation energy term. It is worth noticing that exchange terms are obtained from Eq. (11) at $\gamma = 0$. In the case of $f_{ll} \gg T_{LL}$

$$E_c^s = -\frac{1}{2} f_{ll}^0 Q_l \left(1 - \frac{Q_l}{N_l} \right) + O \left(\frac{T_{LL}}{f_{ll}} \right), \quad (14) \\ V_{cl}^s = \frac{\delta E_c^s}{\delta Q_l} = -\frac{1}{2} f_{ll}^0 \left(1 - 2 \frac{Q_l}{N_l} \right) + O \left(\frac{T_{LL}}{f_{ll}} \right).$$

In Fig. 1 the dependence of E_c^s on Q_d for the model with N_d -fold degeneration of bands and semicircular density of states $g(\varepsilon) = 2WN_d/\pi\sqrt{1 - (\varepsilon/W)^2}$ is presented for several f_{ll}^0/W values. The maximum value of $(-E_c^s)$ is in the middle of the row as it should be and $V_{cl}^s = \delta E_c^s / \delta Q_l$ has maxima at the ends of the interval and is zero in the middle of the row as in Eq. (15).

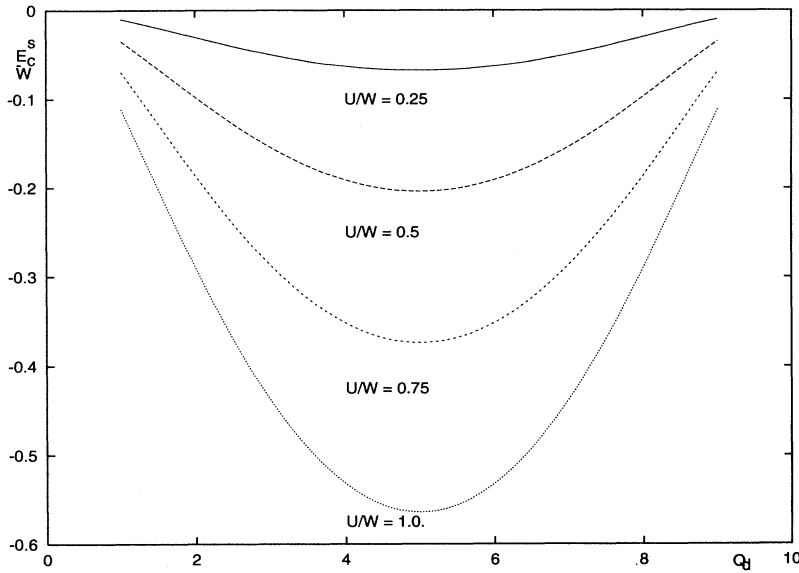


FIG. 1. Correlation energy E_c^s as a function of the number of electrons for a model with the $N_d = 10$ band degeneracy and semi-circular density of states.

Summarizing the above discussion we can note that as soon as we started with Eq. (7) the correlation energy of such a Hamiltonian can be found by various approximation methods, in particular by the Gutzwiller approximation. In the paramagnetic case it is a functional of Q_l —the number of electrons with orbital momentum l . These approximations can in principle be tested and the accuracy of the approximations can be estimated. Most problems arise at the moment when we try to form the Hamiltonian in Eq. (7) from the full long-distance interaction Hamiltonian.

C. The partition between on-site correlations and LDA correlations

The first problem is the exchange diagram. Due to the long-distance nature of the Coulomb interaction, the contribution of neighboring unit cells is considerable both in the free electron gas and in d metals. Several techniques were developed for accurate calculations of such contributions.^{16,17} But in any case the effective interaction due to exchange is large and it embraces several neighboring sites. On the other hand, we believe that the main effect missed in the LDA is the correlation due to the strong on-site repulsion. Thus we should either increase the radius of effective interaction in our model by the inclusion of nearest neighbors or use only the correlation part of the energy in Eq. (11). The first variant is more logical, but the second is simpler, and will be used in calculations below. The exchange contribution will be included in the LDA.

The second problem concerns screening effects. As shown in Sec. III, the SRC contribution E_c^s is quite small in the free electron gas in comparison with the whole correlation energy E_c^{hom} of the homogeneous gas, which is mainly due to screening effects. These effects arise in the particle-hole channel and are not included in the Hub-

bard model, which is a model of neutral electrons. To imitate these effects it seems natural to use a screened interaction

$$V_\lambda(r) = \exp(-\lambda r)/r; \quad \lambda^2 = \min\{p_F^2, 4\pi\Pi(0)\}. \quad (15)$$

$\Pi(0)$ is the polarization operator for the free homogeneous gas with the density $\sum_l Q_l/\Omega$. It is evidently unsatisfactory for calculating the screening correlation energy E_c^{hom} , where the dependence of $\Pi(\omega, \mathbf{k})$ on ω and \mathbf{k} is important, but can be a reasonable approximation for the calculation of short-ranged E_c^s . In essence we adopted the same point of view as in the work of Steiner *et al.*,⁶ that the degrees of freedom corresponding to all the orbitals outside our minimal set $\phi_l(r)$ are integrated out and effectively cause screening of the initial Coulomb interaction. The results obtained are not very sensitive to the choice of λ , as can be seen from Sec. III. For this reason no attempts were made to fit λ values. An example of the first-principles V_λ calculation is presented in Appendix C. It gives λ in the interval 0.5–1.0 for Cu, and 1.2–0.9 for Mn. But even with $V_\lambda(r)$ the interaction cannot be cut down in the boundaries of one unit cell. In real metals λ is about one a.u. and does not prevent the electrons near the Wigner-Seitz boundary from interacting with their counterparts in the neighboring cells. As a consequence in Eq. (7) terms arise corresponding to interaction with neighboring lattice sites. To check the independence of E_c^s on λ the interaction with neighboring sites should be included. But the increase of the interaction radius strongly enlarges the subspace dimension in Eq. (8) and to avoid it the following suggestion was adopted. With the multipole moments neglected, the general Hamiltonian is $\hat{H}_{\text{int}} = \hat{H}_{\text{int}}(R=0) + \sum_{\mathbf{R}} \hat{Q}_0 \hat{Q}_{\mathbf{R}}/R$ with $\hat{Q}_{\mathbf{R}} = \sum_l \hat{Q}_l \mathbf{R}_l$. In any approximation which treats Q fluctuations at different pairs of sites as independent, $E_c = E_c^s(0) + E_c^{\text{long}}$. On the other hand, E_c^{long} depends on the fluctuations of

the whole charge $Q_{\mathbf{R}}$ which in this case is the same in a metal and in the free gas of the same density. With this assumption

$$E_{\text{corr}} = E_c^s + E_c^{\text{hom}} - E_c^{s\text{hom}}, \quad (16)$$

where E_c^s and $E_c^{s\text{hom}}$ are calculated with the same interaction (15). The form of potential (15) is also convenient for calculations, as it permits simple decomposition over angular momentum.

Finally, some remarks are made concerning the \mathbf{k} dependence of MTO's. Due to this dependence some averaging over \mathbf{k} should be done to make the factorization in Eq. (7) on Q_l and the constants $f_{ll'}^L$ possible. From consideration of the lowest-order perturbation theory diagrams it is clear that exchange and correlation terms contain various combinations of $\Psi_{\mathbf{k}}^L$ and $\theta_{\mathbf{k}}^L$. As the exchange contribution is treated through the LDA, the combination

$$|\phi_l(\mathbf{r})|^2 = \sum_{\mathbf{k}} \theta_{\mathbf{k}}^L |\Psi_l^{\mathbf{k}}|^2 / q_l \quad (17)$$

was used to calculate $f_{ll'}^L$, which is closer to the combination arising in the charge-charge correlation channel.

The third problem is the problem of core-valence partitioning for many-body interactions. As noted in Ref. 18, "any calculation, following core-valence partitioning can never be better than the accuracy, with which the interactions between core and valence electrons have been treated." In the LDA scheme the density of the correlation energy $\varepsilon_c(\rho_a(\mathbf{r}))$ is defined with the full density $\rho_a(\mathbf{r})$ which is the sum $\rho_a(\mathbf{r}) = \rho_v(\mathbf{r}) + \rho_c(\mathbf{r})$ of valence $\rho_v(\mathbf{r})$ and core $\rho_c(\mathbf{r})$ densities. $\varepsilon_c(\rho_a(\mathbf{r}))$ especially in 3d metals differs from $\varepsilon_c(\rho_v(\mathbf{r})) + \varepsilon_c(\rho_c(\mathbf{r}))$. On the other hand we seek for valence electron correlation effects. The easiest way to balance the conflicting items is to include ρ_c into the free gas term in Eq. (16). The final expression for the interaction energy is

$$E_{ee} = \frac{1}{2} \int \frac{\rho(\mathbf{r})\rho(\mathbf{r}')}{|\mathbf{r} - \mathbf{r}'|} d^3r d^3r' + \int \varepsilon_x(\rho_a(\mathbf{r}))\rho_a(\mathbf{r})d^3r + E_c^{\text{hom}} \left[\rho_c + \frac{Z}{\Omega} \right] + E_c^s[Q_l, f_{ll'}^0] - E_c^{s\text{hom}}[Z], \quad (18)$$

$$\varepsilon_x(\rho) = -\frac{3}{4}(3/\pi\rho)^{1/3},$$

$$E_c^{\text{hom}}[\rho] = \int d^3r \varepsilon_c(\rho(\mathbf{r}))\rho(\mathbf{r}),$$

and the usual approximation for homogeneous gas correlations is taken for $\varepsilon_c(\rho)$. E_c^s is the correlation energy from Eq. (13) with $f_{ll'}^s$, which are calculated in the potential (15). The corresponding term for the free gas was calculated with $f_{ll'}^{0\text{hom}}$ from LMTO-ASA calculations of the free gas.

At this stage the energy is expressed as a functional of density, occupation numbers, and wave functions (through $f_{ll'}^0$). To close the iteration loop we need a potential to calculate these quantities. The natural choice

is the minimization of $E_0 + E_{ee}$ over coefficients $a_{\mathbf{k}L}^{\nu}$ of the wave-function decomposition over the basic wave-functions ϕ_l . In turn, the functions ϕ_l are the solution of Eq. (2) with $U(r)$ in the LDA approximation. Such a scheme is often used in Hartree-Fock calculations by LMTO or by linearized augmented-plane-wave (LAPW) methods.^{16,17} Some remarks should be made in connection with such an approach.

D. Effective potential in the SRC approach

The density functional can be introduced by various approaches. We shall briefly discuss one of the possibilities, which is the consequence of a rather general minimization principle. Let us suppose that we succeeded in finding the exact interaction energy $E_{\text{int}}[s_{0i}]$ in the field of several external potentials V_{ei} through the set of collective variables $s_{0i} = \langle \Psi_0 | \hat{s}_i | \Psi_0 \rangle$ where $|\Psi_0\rangle$ is the ground state for the system of noninteracting electrons in the external potential V_{ei} : $s_{0i} = \frac{\delta E_0[V_{ei}]}{\delta V_{ei}}$. Then it is convenient to modify the initial ground state $|\Psi_0\rangle$ by adding the terms $\sum_i J_i \hat{s}_i$ to \hat{H}_0 and subtracting them from \hat{H}_{int} :

$$E = E_0[V_i] - \sum_i J_i s_{0i} + E_{\text{int}}[s_{0i}, J_i],$$

where E_{int} now depends on both s_{0i} and J_i , $V_i = V_{ei} + J_i$. The \hat{s}_i mean value s_i is

$$s_i = \frac{\delta E}{\delta V_{ei}} = s_{0i} + \left(\frac{\delta E_{\text{int}}}{\delta s_{0i}} - J_i \right) \frac{\delta s_{0i}}{\delta V_i}$$

and the independence of \hat{H} on J_i gives

$$0 = \left(\frac{\delta E_{\text{int}}}{\delta s_{0i}} - J_i \right) \frac{\delta s_{0i}}{\delta V_i} + \frac{\delta E_{\text{int}}}{\delta J_i} \Big|_{s_{0i}}.$$

It is convenient now to choose

$$J_i = \frac{\delta E_{\text{int}}}{\delta s_{0i}}, \quad (19)$$

as such a choice gives several advantages. First, quantities depending on s_i can be calculated either by direct averaging over the ground state of noninteracting electrons or by the variation of the whole energy over the external potential. Secondly, in the case of the approximate expression $E_{\text{int}}^{\text{appr}}$ for $E_{\text{int}} = \bar{E}_{\text{int}}^{\text{appr}} + \Delta$, this condition automatically minimizes the Δ value. The procedure was used for finding a closed expression for the density functional¹⁹ through the set of skeleton diagrams for E_{int} . In this case s_i is the electron density $n(\mathbf{r})$ and J_i is the DF potential. The Luttinger functional²⁰ for the "dressed" Green function is another example, where s_i corresponds to $G(\mathbf{k}, \omega)$, J_i corresponds to the self-energy $\Sigma(\mathbf{k}, \omega)$, and E_{int} is symbolically expressed through the set of skeleton diagrams. The same principle is used in alloys to create the cluster decomposition of the free energy in cluster variation method and similar approaches.²¹ Below it will be used for finding the form of the DF-like functional in strongly correlated systems.

Thus, if we believe that in our system the interaction of certain collective variables is of importance, we should introduce the corresponding potential, in particular, $V_{cl}^s = \delta E_c^s / \delta Q_l$ in the case of the Hubbard system. In a rigorous sense the functional thus obtained is not a density functional, as it depends on partial density $\rho_l(r)$ (or its integral Q_l), but it is created following the usual procedure, described above. It should truly reproduce not only the density $\rho(r)$, but also occupation numbers Q_l .

There are at least two possibilities to create the effective potential: to vary over occupation numbers and over the wave function $\phi_l(r)$. Let us first consider the case of the variation only over Q_l . In this case $\phi_l(r)$ can be taken as the solution of the Schrödinger equation in a suitable potential, for example, in the potential $U(r) = V_H(\rho_a) + V_x(\rho_a) + V_c(\rho_a)$. After variation of Eq. (18) over Q_l with $|\phi_l(r)|^2$ from Eq. (17), we obtain the secular equation for $a_{\mathbf{k}L}^\nu$:

$$\sum_{L'} \langle \Psi_{L'}^{\mathbf{k}}(r) | \hat{T} + V_H + V_x | \Psi_{L'}^{\mathbf{k}} \rangle a_{\mathbf{k}L}^\nu + (V_{cl}^s + V_c^\alpha - V_c^{shom}) a_{\mathbf{k}L}^\nu = \varepsilon_{\mathbf{k}}^\nu a_{\mathbf{k}L}^\nu, \quad (20)$$

where

$$V_H(r) = -Z_{nucl}/r + \int \rho(r') / |\mathbf{r} - \mathbf{r}'| d^3r',$$

$$V_x(r) = -[3/\pi\rho_a(r)]^{1/3},$$

and V_c^α is the value of the correlation contribution to the chemical potential averaged over a unit cell: $V_c^\alpha = 1/\Omega \int \mu_c(\rho_c + Z/\Omega) d^3r$. The constant V_{cl}^s is the contribution due to on-site repulsion and $V_c^{shom} = \delta E_c^{shom} / \delta Z$. Rewriting Eq. (20) with Eqs. (2) and (3) we obtain

$$\sum_{L'} [H_{LL'}^{\mathbf{k}} + (V_{cl}^s - V_c^{shom} + V_c^\alpha - \mu_{cl}^{\mathbf{k}}) \delta_{LL'}] a_{\mathbf{k}L}^\nu = \varepsilon_{\mathbf{k}}^\nu a_{\mathbf{k}L}^\nu, \quad (21)$$

where $\mu_{cl}^{\mathbf{k}} = \hat{W}^{-1} (\sum_{\alpha, \beta=0,1L''} h_{LL''}^{\alpha\mathbf{k}+} \mu_c^{\alpha\beta} h_{L''L'}^{\beta\mathbf{k}}) \hat{W}^{-1+}$ and $\mu_c^{\alpha\beta} = \int \phi_l^\alpha(r) \mu_c(\rho_a) \phi_l^\beta(r) dr$. The ε_l value in Eq. (2) usually is chosen in such a way that

$$\sum_{\nu\mathbf{k}} h_{LL'}^{\mathbf{k}} a_{\mathbf{k}L}^{*\nu} a_{\mathbf{k}L}^\nu \theta_{\mathbf{k}}^\nu = 0 \quad (22)$$

to diminish nonlinear corrections. With the same condition we obtain from Eqs. (2) and (21) after summation over \mathbf{k}

$$q_l \varepsilon_l = \sum_{\mathbf{k}} \varepsilon_{\mathbf{k}}^\nu \theta_{\mathbf{k}}^\nu a_{L\mathbf{k}}^{*\nu} a_{L\mathbf{k}}^\nu - V_l Q_l \quad (23)$$

where V_l are the shifts between the SRC potential and $U(r)$ averaged over the unit cell volume with the $|\psi_l|^2$. V_l value can be considered as a measure of spectrum deformation in comparison with the LDA approach:

$$V_l = V_{cl}^s - V_c^{shom} + V_c^\alpha - \frac{\sum_{\alpha\beta} q_l^{\alpha\beta} V_l^{\alpha\beta}}{Q_l},$$

$$V_l^{\alpha\beta} = \int \phi_l^\alpha(r) \mu_c(r) \phi_l^\beta(r) dr, \quad (24)$$

and $q_l^{\alpha\beta}$ were defined previously. Equations (18), (21), (23), and (24) are the basic equations for the first variant.

In the second variant the variation over Q_l should make the secular equation for $a_{\mathbf{k}L}^\nu$ and the variation in $\phi_l(\varepsilon, r)$ the potential in Eq. (2). We shall follow the procedure used in the LMTO-ASA method for the DF approach. In the latter case Eq. (2) can be obtained if we vary E_{XC}^{LDA} over the function $\phi_l(\varepsilon, r)$ and afterwards fix ε by any reasonable condition, for example, by the condition (22). In the SRC approach we obtain in Eq. (2)

$$U(r) = V_H(r) + V_x(r) + V_{fl}(r) + V_c^{hom} - V_c^{shom},$$

$$V_{fl}(r) = \frac{1}{Q_l} \frac{\delta E_c^s}{\delta f_{fl}^0} \int_0^{R_{ws}} \frac{1}{r'} |\overline{\phi_{l'}(r')}|^2 dr', \quad (25)$$

with the $|\overline{\phi_{l'}(r')}|^2$ from Eq. (17). For $a_{\mathbf{k}L}^\nu$ we obtain the secular equation

$$\sum_{L'} [H_{LL'}^{\mathbf{k}} + (V_{cl}^s \delta_{LL'} - \langle V_{LL'}^{\mathbf{k}} \rangle)] a_{\mathbf{k}L}^\nu = \varepsilon_{\mathbf{k}}^\nu a_{\mathbf{k}L}^\nu \quad (26)$$

with

$$\langle V_{LL'}^{\mathbf{k}} \rangle = \sum_{\alpha\beta\{L_i\}} (\hat{W}^{-1})_{LL_i} h_{L_i L_2}^{+\alpha\mathbf{k}} V_{fl_2}^{\alpha\beta} h_{L_2 L_3}^{\beta\mathbf{k}} (W^{+-1})_{L_3 L'}$$

and

$$q_l \varepsilon_l = \sum_{\mathbf{k}} \varepsilon_{\mathbf{k}}^\nu \theta_{\mathbf{k}}^\nu a_{L\mathbf{k}}^{*\nu} a_{L\mathbf{k}}^\nu - V_{cl}^s Q_l + \sum_{\alpha\beta} q_l^{\alpha\beta} V_{fl}^{\alpha\beta}, \quad (27)$$

$$V_{fl}^{\alpha\beta} = \int \phi_l^\alpha(r) V_{fl}(r) \phi_l^\beta(r) dr.$$

Equations (18), (21), and (23) for the first variant and (18), (25), and (26) for the second variant make the self-consistent scheme which will be used below for transition metal ground state energy calculations.

III. RESULTS AND DISCUSSION

Paramagnetic phase ground state energy calculations by the LMTO-ASA method were carried out for the 3d metals V, Mn, Ni, and Cu and the 4d metals Nb and Tc. In a sense, these metals are the most significant: Mn is in the middle of the row and the correlation effects due to on-site repulsion should be revealed most completely. As is well known, Mn paramagnetic state calculations give the value of the equilibrium unit cell volume Ω_0 and bulk modulus B with an error extraordinary for this approach, when compared with the experimental ones: 15% in Ω_0 and approximately three times in B .^{22,23} Of course, the Mn ground state at $T = 0$ has a complex antiferromagnetic structure and antiferromagnetic phase calculations give experimental B values, though Ω_0 values are still

TABLE I. Unit cell equilibrium volume Ω (a.u.) and bulk module B (Mbar) calculated by various methods. Values in the LSDA and CGA columns are taken from Ref. 23. The experimental values taken from Ref. 23 are given for comparison. Values in the LDA and SRC columns are the results of the present work.

Metal	Ω	Ω	Ω	Ω	Ω	B	B	B	B	B
	LSDA	CGA	LDA	SRC	expt.	LSDA	CGA	LDA	SRC	expt.
V	89.2	93.1	92.5	99.8	94.6	2.0	1.9	2.2	1.5	1.6
Mn	71.6	79.6	76.2	83.4	85.6 ^a	3.1	2.8	2.8	1.8	1.3
Ni	69.6	75.2	71.8	86.0	73.8	2.9	2.5	1.5	1.1	1.8
Cu			77.4	76.8	83.0			1.3	1.9	1.1
Nb	123.8	130.5	133.1	134.1	121.5	1.8	1.7	2.8	2.7	1.8
Tc	100.1	104.2	105.1	107.2	96.8	3.1	2.8	3.4	4.2	2.8

^aData from Ref. 24.

lower than in experiment.²² But small additions of impurities or variations of either temperature or pressure make the paramagnetic ground state with the fcc structure; meanwhile, the variation of either Ω_0 or B at such a transition does not exceed 10%.²⁴ For example, the interpolation of results on $B(x)$ dependence in $\text{Mn}_{1-x}\text{Cu}_x$ alloys²⁴ gives a B value at $x = 0$ close to that in the antiferromagnetic phase. Thus the problem of unusually low values of B and the difference in Ω in the paramagnetic state still exists and below it will be argued that one of the possible explanations consists in the influence of strong electron correlations. Qualitatively, the effect was discussed in Ref. 25. In V, the values of the “Hubbard” constant U from Eq. (1) are less than that in Mn and the number of d electrons is less too. Both these factors diminish the value of correlation effects and V LDA calculations reproduce experimental values fairly well. In Cu the U value is extremely large, but the number of d holes is small and a reasonable technique should bring on small correlation effects. Ni is a strong ferromagnet and large correlation effects are expected. Nb and Tc are the V and Mn analogs and again the accurate approach should give tiny corrections to the LDA values. Briefly, Mn is the metal where correlation effects should give noticeable corrections to the LDA, and the other metals can be considered as a test for the disappearance of correlation effects.

In Table I the results of LDA and SRC calculations are listed and compared with the experiment and the results of other authors. The calculations were performed with a frozen core. In all the metals the constant λ in the potential from Eq. (15) was chosen to be 1.0 without attempts to fit it. For comparison, in Mn for $\lambda = 1.0, 0.5,$ and 0.3 we obtain $\Omega = 83.4, 86.8,$ and 87.7 and $B = 1.8, 2.0,$ and 2.1 , though the f_{II}^0 values change by a factor of two. For $\lambda = 1.0$ and 0.5 we obtain $\Omega = 86.0$ and 81.1 in Ni and $\Omega = 76.8$ and 75.8 in Cu. Both variants for preparation of the effective potential were tested. In Mn and V and $4d$ metals Nb and Tc they give similar results, but in Ni and Cu the first variant fails, as the inhomogeneity of the d function in these metals is strong and the “smeared” constant potential of the first variant significantly differs from the LDA and the potential of the second variant. The results, listed in Table I, were obtained with Eqs. (18), (25), and (26), i.e., in the second variant. Ω_0 and

B values were obtained by least-square fitting of results obtained for Ω values in the vicinity of Ω_0 . The general trends coincide with the above-mentioned consideration of the correlation effect significance. To clarify the mechanism of increasing Ω_0 and smearing of the bulk modulus B we present in Table II the values of E_c^s [Eq. (13)], and its volume derivative $p_c = -dE_c^s/d\Omega$, obtained by numerical differentiation of $E_c^s(\Omega)$. In addition, the values of ξ_l parameters are presented, which show the extent of the band “dynamical” narrowing and the significance of correlation effects in accordance with Eq. (13). For noninteracting electrons $\xi_l = 1.0$. These quantities add very little to the LDA results in all the metals except Mn. In Mn p_c shifts the equilibrium volume by approximately 10 a.u., when added to the LDA results. The strong dependence of E_c^s on Ω and large ξ_d value in Mn appear to approve the following mechanism of B softening: the strong dependence of correlation energy on the unit cell volume Ω permits this value to play the role of an adjustable parameter, i.e., the correlation function, proportional to $\langle(Q - \langle Q_l \rangle)^2\rangle$, changes so that it partly recovers the increase in total energy and as a consequence the metal becomes more pliant. The increase of kinetic energy $-T_{LL}^k(1 - \xi_l^2)$ due to ξ_l moves the equilibrium volume to larger values, similarly to the ferromagnetic case as the increase is smaller for larger R_{WS} values. In this connection it is interesting to compare quasiparticle spectra in the SRC and LDA. In Fig. 2 the Mn electronic structure obtained by both methods is presented. Both electronic spectra are quite similar.

In Table III values of $V_{cl}^s, V_c^{shom},$ and V_l from Eq. (20) are listed. It is worth noticing the small values of the

TABLE II. The renormalization factor ξ_l [Eq. (12)], correlation energy E_c^s (a.u.), and its volume derivative $p_c = -dE_c^s/d\Omega$ (Mbar) for some transition metals.

Metal	Ω (a.u.)	ξ_s	ξ_p	ξ_d	E_c^s	p_c
V	96.4	0.975	0.983	0.956	-0.096	0.047
Mn	85.8	0.971	0.978	0.898	-0.184	0.159
Ni	79.2	0.973	0.981	0.853	-0.112	0.034
Cu	79.2	0.996	0.997	0.985	-0.007	-0.061
Nb	128.6	0.987	0.992	0.989	-0.035	-0.003
Tc	103.9	0.985	0.988	0.977	-0.066	-0.005

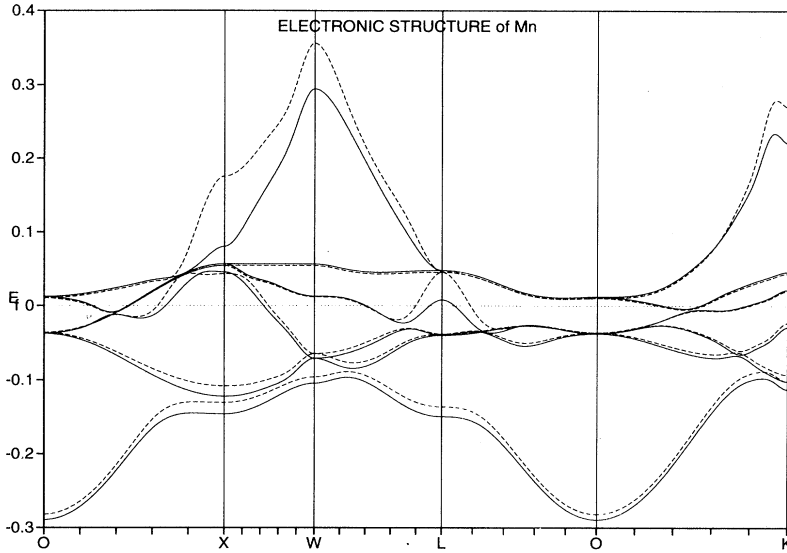


FIG. 2. The dependence of $\epsilon_{\mathbf{k}}^{\nu}$ (a.u.) on \mathbf{k} along symmetry lines in Mn. Solid line represents LDA and dashed line represents SRC calculations.

homogeneous gas on-site correlation potential V_c^{shom} . It correlates with the small value of the correlation on-site energy E_c^{shom} in the homogeneous gas in comparison with its whole correlation energy E_c^{hom} , which is mainly due to screening effects. For example, for the density 7/85 a.u. that approximately corresponds to Mn, $E_c^{shom} = -0.02$ a.u. Meanwhile $E_c^{hom} = -0.36$ a.u. All the values in Table III were obtained with the $\phi_l(r)$ calculated in the LDA potential. The V_l in this case is completely determined by the difference in correlation LDA potential of the inhomogeneous gas and the sum of the homogeneous gas potential and correlation potential due to on-site repulsion V_{cl}^s . In V, Nb, and Tc V_{cl}^s is small, as all the Hubbard-like correlations are small. But even in Mn this quantity is small in spite of large values of correlation energy E_c^s . It is in agreement ($Q_l \approx N_l/2$) with the dependence of V_{cl}^s from Eq. (14) and is also supported by numerical calculations in a semicircular model for small U . As a result, the values of energies corresponding to the center of gravity for subbands with a particular l are practically the same as in the LDA. These values are listed in Table IV. They practically coincide in SRC I (variation over Q_l only) and SRC II approaches [variation over both Q_l and $\phi_l(r)$]. This means that the main effect is due to the variation of occupation numbers. On the con-

trary, in Cu, the correlation energy value is small, but the potential V_{cl}^s is large, though it turns out to be smaller than expected from comparison with the U value. But in Cu the difference between the correlation potential of the inhomogeneous gas and that of the homogeneous gas is noticeable and partly compensates the large V_{cl}^s values. Nevertheless, the difference between SRC I and SRC II is large. All the data are presented at one and the same unit cell volume Ω . Of course, equilibrium volumes in the LDA and SRC differ. As a last example, in Table V the values of $f_{ll'}^0$ parameters for various λ values are listed for V, Mn, Ni, and Cu. Though these values strongly depend on λ , the U value Eq. (1), which is the measure of correlation effects, is approximately constant. Moreover, though absolute values of E_c^s vary strongly with λ , which is quite natural, p_c varies much less. Summarizing the presented results, we can note that strong on-site electron correlations cause large correlation energy corrections in the middle of the d -metal row and these corrections bring the values of the calculated equilibrium unit cell volume and bulk modulus to their experimental values.

IV. CONCLUSION

In this paper a method for incorporating strong correlation effects in *ab initio* ground state energy calculations is presented. Starting from a ‘‘Hubbard-like’’ Hamiltonian we obtain the correlation energy in the Gutzwiller approximation as a functional of partial occupation numbers Q_s , Q_p , and Q_d . The exchange energy is considered in the LDA approximation and the part of the correlation energy due to particle-hole pairs is taken as that in the homogeneous electron gas of the same density. With these assumptions, the functional (13) and (18), which can be considered as a generalization of the DF, is obtained. Two possible LMTO-ASA-based approaches are considered: the variation of coefficients in the wave-

TABLE III. The values (in eV) of the free electron gas potential V_c^{shom} , correlation potentials V_{cl}^s , and differences in values of potentials V_l [Eq. (24)] between the LDA and SRC. Ω values are the same as in Table II.

Metal	V_c^{shom}	V_{cs}^s	V_{cp}^s	V_{cd}^s	V_s	V_p	V_d
V	-0.03	-0.38	-0.41	-0.35	-0.05	-0.49	-0.92
Mn	0.03	-0.30	-0.41	0.33	-0.22	-0.54	-0.52
Ni	0.11	-0.22	-0.33	2.86	-0.36	-0.62	1.63
Cu	0.14	-0.14	-0.24	2.71	-0.38	-0.62	1.42
Nb	-0.03	-0.28	-0.30	-0.14	0.11	-0.41	-0.41
Tc	0.08	-0.28	-0.35	0.11	-0.05	-0.49	-0.41

TABLE IV. Energies (in a.u.) corresponding to the center of gravity for subbands with various l . Unit cell volumes are the same as in Table II.

Metal	LDA			SRC I ^a			SRC II ^b		
	ϵ_s	ϵ_p	ϵ_d	ϵ_s	ϵ_p	ϵ_d	ϵ_s	ϵ_p	ϵ_d
V	-0.156	-0.081	-0.071	-0.170	-0.101	-0.090	-0.167	-0.095	-0.085
Mn	-0.200	-0.123	-0.099	-0.213	-0.138	-0.112	-0.216	-0.143	-0.116
Ni	-0.241	-0.166	-0.119	-0.253	-0.165	-0.100	-0.265	-0.193	-0.140
Cu	-0.247	-0.171	-0.146	-0.261	-0.176	-0.124	-0.269	-0.210	-0.235
Nb	-0.150	-0.076	-0.080	-0.161	-0.088	-0.091	-0.158	-0.084	-0.086
Tc	-0.179	-0.098	-0.100	-0.191	-0.111	-0.112	-0.200	-0.123	-0.122

^aCalculations on the basis of Eqs. (18) and (21).

^bCalculations on the basis of Eqs. (18) and (26).

function decomposition over MTO's only and the variation of both coefficients and MTO's. Both approaches give similar results for all metals but Ni and Cu, where the second approach is more favorable. The SRC results are close to the LDA DF results for the majority of transition metals except Mn. In the latter case the equilibrium unit cell volume and bulk modulus are significantly improved when compared with the experiment. We consider mainly ground state calculations and in this way we differ from analogous work,⁶ where the attention was focused on the excitation spectra of strongly correlated systems. The use of the Gutzwiller approximation instead of the approximation of Ref. 8 is the other difference from Ref. 6.

Let us discuss perspectives of the present approach. This work appears to be only the first step towards subsequent incorporation of correlation effects in electronic structure calculations. Further improvement should take into account the screening effects and effects due to repulsion simultaneously. For these purposes, as is seen from Secs. II and III and Appendix C, the form of the model Hamiltonian should include both the interactions with the neighboring sites, and as a consequence a cluster approximation for E_c^s is needed. Calculations of the charge distribution around an impurity²⁶ show that the charge is completely screened by first neighboring atoms and thus the size of the cluster need not be extremely large. Ei-

ther extended Gutzwiller or other approximations, such as the coupled-cluster method (CCM)²⁷ can be useful for treating on-site correlations and screening effects on the same footing. Moreover, the effects of screening appear to dominate in investigation of excitation spectra. For example, the comparison of the spectra with experiment for Fe-Ni systems⁶ shows that the "first-principles" U should be significantly diminished to reproduce the experiment. While we confine ourselves to a one-site model Hamiltonian and one-site cluster, these effects can hardly be considered self-consistently.

ACKNOWLEDGMENTS

The author is indebted to M. I. Katsnelson, E. G. Maksimov, and Yu. Ch. Vekilov for useful discussions. The work was supported by the International Scientific Foundation under Grant No. RGQ000 and by the Russian Fund of Fundamental Research under Grant No. 93-02-14776.

APPENDIX A: LMTO-ASA MATRIX ELEMENTS

Below, the LMTO-ASA formulas¹⁴ used in the present work are listed for references and definition. The h_{LL}^k matrix in Eq. (3) is expressed in terms of the matrices $\hat{\omega}(-)$, $\hat{\Delta}$, $\hat{\gamma}$, and matrix of structure constants \hat{S}^k :

$$\hat{h}^k = \hat{\omega}(-) - \hat{\Delta} \hat{S}^k \frac{1}{1 - \hat{\gamma} \hat{S}^k} \hat{\Delta}. \quad (A1)$$

The matrix elements of these matrices are expressed through the values of the wave functions at the Wigner-Seitz radius $\phi_{lR} = \phi_l(R_{WS})$. The matrices $\hat{\omega}(-)$, $\hat{\Delta}$, and $\hat{\gamma}$ have the diagonal form

$$\begin{aligned} \omega_l(-) &= -\frac{-l\phi_{lR} - R_{WS}\phi'_{lR}}{-l\dot{\phi}_{lR} - R_{WS}\dot{\phi}'_{lR}}, \\ \omega_l(+) &= -\frac{(l+1)\phi_{lR} - R_{WS}\phi'_{lR}}{(l+1)\dot{\phi}_{lR} - R_{WS}\dot{\phi}'_{lR}}, \\ \phi_l(\pm) &= \phi_{lR} + \omega(\pm)\dot{\phi}_{lR}, \end{aligned} \quad (A2)$$

$$\Delta_l = \sqrt{\frac{\phi_l^2(-)}{4R_{WS}}}, \quad \gamma_l = \frac{\phi_l(-)}{2(2l+1)\phi_l(+)}.$$

TABLE V. The values (in eV) of interaction constants $f_{ll'}^0$ and Hubbard constant U [Eq. (1)] for some values of the screening constant λ in Eq. (15).

Metal	λ	f_{ss}	f_{pp}	f_{sd}	f_{dd}	U
V	1.0	3.14	2.02	2.75	3.85	1.49
Mn	1.0	2.61	1.95	2.44	6.10	3.83
Mn	0.5	4.76	4.44	5.31	9.87	3.92
Mn	0.3	6.90	6.44	7.87	12.51	3.67
Mn	0.0	11.67	11.44	13.27	20.27	5.50
Ni	1.0	2.44	1.80	2.92	9.67	6.17
Ni	0.5	4.58	4.10	5.68	13.78	7.00
Cu	1.0	2.39	1.71	2.96	10.90	7.37
Cu	0.5	4.58	3.67	5.64	14.79	8.09
Cu	0.0	12.05	11.56	13.94	25.11	9.28
Nb	1.0	2.49	1.55	1.94	1.94	0.55
Tc	1.0	2.44	1.80	2.22	2.97	0.97

The $\hat{H}^{\mathbf{k}}$ matrix can be expressed in terms of $\hat{h}^{\mathbf{k}}$:

$$\begin{aligned}\tilde{H}_{LL'}^{\mathbf{k}} &= \varepsilon_l \delta_{LL'} + h_{LL'}^{\mathbf{k}} + \sum_{L''} h_{LL''}^{\dagger \mathbf{k}} \varepsilon_{l''} \langle \dot{\phi}_{l''}^2 \rangle h_{L''L}^{\mathbf{k}}, \\ \hat{H} &= \hat{W}^{-1} \tilde{H} \hat{W}^{+1},\end{aligned}\quad (\text{A3})$$

where the \hat{W} matrix is defined by the decomposition of the overlap matrix \hat{O} :

$$\begin{aligned}O_{LL'}^{\mathbf{k}} &= \delta_{LL'} + \sum_{L''} h_{LL''}^{\dagger \mathbf{k}} \langle \dot{\phi}_{l''}^2 \rangle h_{L''L}^{\mathbf{k}}, \\ \langle \dot{\phi}_{l''}^2 \rangle &= \int_0^{R_w} \phi_l^2(r) dr, \quad \hat{O} = \hat{W} \hat{W}^+.\end{aligned}$$

For brief designation the following definitions are used:

$$\begin{aligned}\phi_l^0(r) &= \phi_l(r), \quad \phi_l^1(r) = \dot{\phi}_l(r), \\ h_{LL'}^{0\mathbf{k}} &= \delta_{LL'}, \quad h_{LL'}^{1\mathbf{k}} = h_{LL'}^{\mathbf{k}}.\end{aligned}\quad (\text{A4})$$

APPENDIX B: CORRELATION ENERGY CALCULATIONS IN THE GUTZWILLER APPROXIMATION

For the case of equal occupancy for states with various m but equal l , $\langle n_{lm} \rangle = Q_l/N_l$, the coefficients of the decomposition of the U operators [Eq. (13)] over \hat{P}_{nm} [Eq. (10)] can be easily found: $\hat{U} = \sum C(n) \hat{P}_{n,N-n}$, where n is the set of numbers of electrons $\{i_l\}$ in s , p , and d states:

$$C(\{i\}) = \exp \left[-\gamma \sum_{l'} f_{l'} (i_l - Q_l) (i_{l'} - Q_{l'}) - \sum_l \mu_l i_l \right]. \quad (\text{B1})$$

Using the Wick theorem in averaging over the ground state $|\Psi_0\rangle$ with the mean occupation numbers $c_l = n_l/N_l$, we obtain for K_0 in Eq. (8)

$$\begin{aligned}K_0 &= \sum_{\{i\}} C(\{i\})^2 F_s F_p F_d, \\ F_l &= \frac{N_l!}{i_l! (N_l - i_l)!} c_l^{i_l} (1 - c_l)^{(N_l - i_l)}.\end{aligned}\quad (\text{B2})$$

Equation (9) takes the form

$$Q_l K_0 = \sum_{\{i\}} i_l C(\{i\})^2 F_s F_p F_d \quad (\text{B3})$$

and for ξ_l in Eq. (10)

$$\xi_l K_0 = \sum_{\{i\}} C(\{i\}) C(\{i'\}) F_s F_p F_d \frac{N_l - i_l}{N_l} \frac{1}{1 - c_l}, \quad (\text{B4})$$

where the set $\{i'\}$ differs from the set $\{i\}$ in one electron added to i_l . After solution of the system of Eqs. (B3) for $\exp(-2\mu_l)$ by the Newton method we find E_c^s with Eq. (B4) and

$$\begin{aligned}\langle (\hat{Q}_l - Q_l)(\hat{Q}_{l'} - Q_{l'}) \rangle \\ = \sum_{\{i\}} C(\{i\})^2 F_s F_p F_d (i_l - Q_l)(i_{l'} - Q_{l'}) / K_0.\end{aligned}\quad (\text{B5})$$

At this step the γ value changes in accordance with the minimization algorithm and the procedure repeats until self-consistency in γ is gained.

APPENDIX C: RENORMALIZED EFFECTIVE INTERACTION

The main purpose of this article is the estimation of correlation effects due to Hubbard-type on-site repulsion in solids. But in real solids Hubbard-type and screening correlations are mixed. For this reason the complete solution of the problem demands calculations in a cluster, which includes several lattice sites. But as the first approximation we can omit interaction with the other lattice sites (as usual in the Hubbard model) and use the effective Hamiltonian, with the effective screened interaction, obtained in the spirit of the GW approach. In the GW approach²⁸ the effective interaction $W(\mathbf{r}, \mathbf{r}', \omega)$ is

$$\begin{aligned}W(\mathbf{r}, \mathbf{r}', \omega) &= V(\mathbf{r} - \mathbf{r}') \\ &+ \int V(\mathbf{r} - \mathbf{r}_1) \Pi(\mathbf{r}_1, \mathbf{r}_2, \omega) \\ &\times W(\mathbf{r}_2, \mathbf{r}', \omega) d^3 r_1 d^3 r_2,\end{aligned}\quad (\text{C1})$$

where $\Pi(\mathbf{r}_1, \mathbf{r}_2, \omega)$ is the polarization operator and $V(\mathbf{r} - \mathbf{r}')$ is the Coulomb interaction. Usually only static interaction with $\omega = 0$ is considered. The main contribution usually gives the RPA diagram for Π , though vertex corrections can change its value by up to 40%:²⁸

$$\begin{aligned}\Pi(\mathbf{r}_1, \mathbf{r}_2, \omega) &= \Pi^h(\mathbf{r}_1, \mathbf{r}_2, \omega) + \Pi^l(\mathbf{r}_1, \mathbf{r}_2, \omega) \\ &= \sum_{\lambda, \mu \mathbf{k} \mathbf{k}'} \Psi_{\lambda \mathbf{k}}^*(\mathbf{r}) \Psi_{\mu \mathbf{k}'}(\mathbf{r}) \Psi_{\mu \mathbf{k}'}^*(\mathbf{r}') \Psi_{\lambda \mathbf{k}}(\mathbf{r}') \\ &\times \frac{\theta_{\mu \mathbf{k}'} - \theta_{\lambda \mathbf{k}}}{\varepsilon_{\lambda \mathbf{k}} - \varepsilon_{\mu \mathbf{k}'}},\end{aligned}\quad (\text{C2})$$

where $\Psi_{\lambda \mathbf{k}}$ are the Bloch eigenfunctions corresponding to the eigenvalue $\varepsilon_{\lambda \mathbf{k}}$. In the LMTO method the low-lying states ν , in particular occupied states, have $\Psi_{\nu \mathbf{k}}(\mathbf{r})$ defined by Eq. (3). The contribution to Π from transitions between these low-lying states is denoted by Π^l . The term Π^h arises due to transitions from occupied states to high-lying empty states. Estimation of Π can be done either by the matrix technique²⁸ with a sufficiently large number of empty states, or by a technique widely used in nuclear physics²⁹ for the same purposes and especially convenient in LMTO method. In this technique Π is rewritten through the Green function:

$$\begin{aligned}\Pi(\mathbf{r}, \mathbf{r}', \omega) &= \sum_{\lambda \mathbf{k}} \theta_{\lambda \mathbf{k}} \Psi_{\lambda \mathbf{k}}^*(\mathbf{r}) \Psi_{\lambda \mathbf{k}}(\mathbf{r}') \\ &\times [G_{\mathbf{k}}(\mathbf{r}, \mathbf{r}', \varepsilon_{\lambda \mathbf{k}} + \omega) + G_{\mathbf{k}}(\mathbf{r}, \mathbf{r}', \varepsilon_{\lambda \mathbf{k}} - \omega)],\end{aligned}\quad (\text{C3})$$

and the Green function in the unit cell is expressed through the combination of regular $\phi(r)$ and irregular $\phi^{\text{irr}}(r)$ solutions of the radial Schrödinger equation with the Wronskian W_L equal to unity. The Green function has poles at $\varepsilon_{\nu\mathbf{k}}$:³⁰

$$G(\mathbf{r} + \mathbf{R}, \mathbf{r}' + \mathbf{R}', \omega) = G^h(\mathbf{r}, \mathbf{r}', \omega) \delta_{RR'} + \sum_{RL, R'L'} \Psi_{RL}^*(\mathbf{r}) G_{RL, R'L'}(\omega) \times \Psi_{R'L'}(\mathbf{r}'),$$

$$G^h(\mathbf{r}, \mathbf{r}', \omega) = \sum_L \frac{\phi_L(\omega, r^<) \phi_L^{\text{irr}}(\omega r^>)}{W_L(\omega)} Y_L(\hat{r}) Y_L(\hat{r}'). \quad (\text{C4})$$

Any combination of regular solutions can be added to ϕ^{irr} , but as was argued in Ref. 30 the choice matching ϕ^{irr} to the boundary condition

$$\left. \frac{d\phi^{\text{irr}}(r)}{dr} \right|_{r=R_{\text{WS}}} = \left. \frac{d\phi(r)}{dr} \right|_{r=R_{\text{WS}}} \quad (\text{C5})$$

corresponds to the case when G^h has no poles at low ω and thus represents the contribution of high levels. For this reason in a crude approximation we can use Eq. (C3) for obtaining Π^h at $\omega = 0$ and with $G = G^h$ from Eq. (C5). The interaction $W(r)$ thus obtained should be used in all the calculations instead of $V(\lambda)$ from Eq. (15). Comparing the two approaches we can estimate λ as

$$\lambda^2 = \frac{32\pi Q_l}{\Omega} \sum_l \int_0^{R_{\text{WS}}} \phi_l(r) \phi_l^{\text{irr}}(\varepsilon_l, r) dr \int_0^r \phi_l^2(\varepsilon_l, r') dr', \quad (\text{C6})$$

where ϕ_l^{irr} obeys the boundary condition (C5). The second term Π^l can be calculated directly with the $\Psi_{\nu\mathbf{k}}$ from Eq. (3). It brings about the renormalization of constants

$$W_{ll'}^0 = V_{ll'}^0 - \sum_{l_1 l_2} V_{ll_1}^0 \Pi_{l_1 l_2} W_{l_2 l'} \quad (\text{C7})$$

with

$$\Pi_{ll'} = \sum_{\lambda, \nu\mathbf{k}\mathbf{k}'} a_{\lambda\mathbf{k}}^{*L} a_{\nu\mathbf{k}'}^L a_{\nu\mathbf{k}'}^{*L'} a_{\lambda\mathbf{k}}^{L'} \frac{\theta_{\nu\mathbf{k}'} - \theta_{\lambda\mathbf{k}}}{\varepsilon_{\lambda\mathbf{k}} - \varepsilon_{\nu\mathbf{k}'}}. \quad (\text{C8})$$

The contribution from Eq. (C6) turns out to be negligible, especially in the middle of the row, in comparison with that from Eq. (C8). Comparing the values obtained from Eq. (C8) with that calculated with the V_λ from Eq. (15) we can estimate the equivalent λ , though the $V_\lambda(r)$ dependence on r is different from that in $W(r)$. The equivalent λ values are ~ 1.0 for V, ~ 1.2 for Mn, and ~ 1.0 for Cu. With the suggestion that the vertex corrections can diminish the Π value by about 40%,²⁸ we would obtain $\lambda = 0.9$ in Mn and $\lambda = 0.5$ in Cu. Thus the reasonable $f_{ll'}^0$ constants correspond to V_λ with λ in the interval 0.5–1.0. The weak dependence of the results on the λ choice permits us to use any λ in the vicinity of that from Eq. (C8) for the estimation of the magnitude of the Hubbard-type correlation effects.

¹ R. O. Jones and O. Gunnarson, Rev. Mod. Phys. **61**, 689 (1989).
² V. I. Anisimov, J. Zaanen, and O. K. Andersen, Phys. Rev. B **44**, 943 (1991).
³ M. T. Czyzyk and G. A. Sawatzky, Phys. Rev. B **49**, 14 211 (1994).
⁴ O. Gunnarson, O. K. Andersen, O. Jepsen, and J. Zaanen, Phys. Rev. B **39**, 1708 (1989).
⁵ M. M. Steiner, R. C. Albers, D. J. Scalapino, and L. J. Sham, Phys. Rev. B **43**, 1637 (1991).
⁶ M. M. Steiner, R. C. Albers, and L. J. Sham, Phys. Rev. B **45**, 13 272 (1992).
⁷ S. V. Beiden, N. E. Zein, and G. D. Samolyuk, Phys. Lett. A **177**, 167 (1993).
⁸ B. Horvatik and V. Zlatic, Solid State Commun. **54**, 957 (1985).
⁹ M. C. Gutzwiller, Phys. Rev. **137**, A1726 (1965).
¹⁰ D. Vollhardt, Rev. Mod. Phys. **56**, 99 (1984).
¹¹ F. Gebhard, Phys. Rev. B **41**, 9452 (1989); **44**, 992 (1991).
¹² S. L. Reindl and G. H. Pestor, Phys. Rev. B **47**, 4680 (1993).
¹³ G. Stollhoff and A. Fulde, Z. Phys. **14**, 3312 (1984).
¹⁴ O. K. Andersen, Phys. Rev. B **12**, 3060 (1975).
¹⁵ B. N. Parlett, *The Symmetric Eigenvalue Problem* (Prentice-Hall, Englewood Cliffs, NJ, 1980).
¹⁶ A. Svane, Phys. Rev. B **35**, 5496 (1987).
¹⁷ S. Massidda, M. Posternak, and A. Baldareschi, Phys. Rev. B **48**, 5058 (1993).

¹⁸ Eric L. Shirley and R. M. Martin, Phys. Rev. B **47**, 15 413 (1993).
¹⁹ L. J. Sham, Phys. Rev. B **32**, 3876 (1985).
²⁰ J. M. Luttinger and J. C. Ward, Phys. Rev. **118**, 1417 (1960).
²¹ J. M. Sanchez, F. Ducastelle, and D. Gratias, Physica A **128**, 334 (1984); V. G. Vaks, N. E. Zein, and V. V. Kamyschenko, J. Phys. F **18**, 1641 (1988).
²² V. L. Moruzzi, P. M. Marcus, and J. Kubler, Phys. Rev. B **39**, 6957 (1989).
²³ H. Körling and J. Häglund, Phys. Rev. B **45**, 13 293 (1992).
²⁴ V. E. Zinoviev, *Metal Kinetic Properties Under High Temperatures* (Metallurgia, Moscow, 1984); Y. Tsumoda, N. Oishi, and N. Kunitomi, J. Phys. Soc. Jpn. **53**, 359 (1984).
²⁵ G. Stollhoff, A. M. Oles, and V. Heine, Phys. Rev. B **41**, 7028 (1990).
²⁶ B. Drittler, M. Weinert, R. Zeller, and P. H. Dederichs, Phys. Rev. B **39**, 930 (1989).
²⁷ R. F. Bishop and K. H. Lüthmann, Phys. Rev. B **26**, 5523 (1982).
²⁸ See, for example, E. L. Shirley and R. M. Martin, Phys. Rev. B **47**, 15 404 (1993); J. E. Northrup, M. S. Hybertsen, and S. G. Louie, Phys. Rev. B **39**, 8198 (1989), and references cited therein.
²⁹ V. A. Khodel and E. E. Saperstein, Phys. Rep. **92**, 183 (1982).
³⁰ O. Gunnarson, O. Jepsen, and O. K. Andersen, Phys. Rev. B **27**, 7144 (1983).